Time-Resolved *In Situ* Spectroelectrochemical Study on Reduction of Sulfur in *N,N′*-Dimethylformamide

Dong-Hun Han,[a] Bum-Soo Kim,[b] Shin-Jung Choi,[a] Yongju Jung,[c] Juhyoun Kwak,[d,*] and Su-Moon Park[a,*,z]

[a]*Department of Chemistry and Center for Integrated Molecular Systems, Pohang University of Science and Technology, Pohang, Gyeongbuk 790-784, Korea*
[b]*UP Chemicals, Pyongtak 459-050, Korea*
[c]*Korea Atomic Energy Research Institute, Nuclear Chemistry Research Division, Daejeon 305-353, Korea*
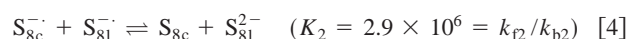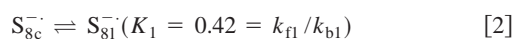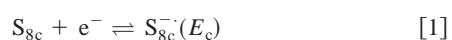[d]*Department of Chemistry, Korea Advanced Institute of Science and Technology, Daejeon 305-701, Korea*

Real-time *in situ* spectroelectrochemical studies have been carried out in *N,N′*-dimethyl formamide containing lithium trifluoromethane sulfonate as an electrolyte and the results are reported. The results indicate that the primary reduction product of the cyclic form of sulfur, S_{8c}^{2-}, undergoes an equilibrium reaction to its linear chain counterpart, S_{8l}^{2-}, which then dissociates into various products. These two dianions and $S_3^{-\cdot}$ were produced along with a minor product, S_4^{2-}, at the potential corresponding to the first electron transfer. These products were further reduced or dissociated to species including S_7^{2-}, S_6^{2-}, S_5^{2-}, S_4^{2-}, S_3^{2-}, S_2^{2-}, and S^{2-} at the second electron-transfer step as evidenced by the spectral shifts observed during electrolysis. The reduction reactions are generally chemically reversible, making it possible to use sulfur reduction as a cathode reaction for Li/S batteries. © 2004 The Electrochemical Society. [DOI: 10.1149/1.1773733] All rights reserved.

Rechargeable lithium batteries have been used as a power source for portable electronic devices because of their high specific energies and high voltages. Although the Li/S systems have been known to provide the highest specific energies among various types of electrochemical cells, the system has not received due attention due to their relatively low operating voltages. Thanks to the recent trend of miniaturization and power requirements in the potable electronic devices, voltage and power consumptions required for the operation of the chips became less stringent. Because low operating voltages are not a problem anymore, the Li/S batteries have recently been reviewed[1,2] and extensive studies have been performed on the electrochemical reduction of sulfur.[3-19] Nevertheless, the electrochemical reduction of sulfur used as a cathode reaction has been known to be complicated, and final products as well as reaction paths have not been elucidated.
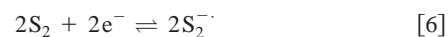
It has been reported that various polysulfides (S_n^{x-}) are generated from electrochemical reduction of cyclooctasulfur (S_{8c}), which is known to be the most stable form of the elemental sulfur.[9,20] The structure of polysulfides could be either cyclic or linear chain form. From theoretical studies, Sahalub *et al.*[20] have reported that the stable structures of S_4^{2-} and S_3^{2-} are the chain form. According to Hunsicker *et al.*,[21] the stable structure of polysulfides depends on the number of S, *n*, in S_n^{x-}; the chain structure is stable when *n* is less than five, whereas cyclic structure is stable when the *n* value is eight or nine. When *n* is six or seven, the polysulfides could have either a cyclic or chain form. Based on chemical, electrochemical, and/or spectroscopic studies, characteristics of various polysulfides have been confirmed and various reduction mechanisms have been proposed as shown later, although they are still highly controversial.

From the simulation of cyclic voltammograms (CVs) obtained at various temperatures and scan rates, Levillain *et al.*[16] proposed the electrochemical reduction mechanism of S_8 in *N,N′*-dimethylformamide (DMF), which consists of a series of electrochemical and chemical reactions

$$S_{8c} + e^- \rightleftharpoons S_{8c}^{-\cdot} (E_c) \quad [1]$$

$$S_{8c}^{-\cdot} \rightleftharpoons S_{8l}^{-\cdot} (K_1 = 0.42 = k_{f1}/k_{b1}) \quad [2]$$

$$S_{8l}^{-\cdot} + e^- \rightleftharpoons S_{8l}^{2-} (E_1 \text{ and } E_1 > E_c) \quad [3]$$

$$S_{8c}^{-\cdot} + S_{8l}^{-\cdot} \rightleftharpoons S_{8c} + S_{8l}^{2-} \quad (K_2 = 2.9 \times 10^6 = k_{f2}/k_{b2}) \quad [4]$$

Here, c and l in the subscripts denote the cyclic and linear chain molecules, respectively. They also asserted that the spectroscopic observation of these species would be difficult during spectroelectrochemical experiments due to the instability of $S_{8c}^{-\cdot}$ and $S_{8l}^{-\cdot}$ species. They obtained the K_1 and K_2 values with $k_{f1} = 212$ s^{-1} and $k_{f2} = 1.4 \times 10^{-6}$ s^{-1}, respectively, at 293 K from digital simulation of CVs.

Based on UV-visible (UV-vis) spectroscopic studies on the electrolyzed solution of sulfur in dimethylacetamide, Bosser and Paris[9] claimed that S_2 molecules were obtained first through partial dissociation of cyclooctasulfur (S_{8c}) and then reduced to generate $S_2^{-\cdot}$. They proposed a somewhat different reaction mechanism from others as follows

$$S_8 \rightleftharpoons 4S_2 \quad [5]$$

$$2S_2 + 2e^- \rightleftharpoons 2S_2^{-\cdot} \quad [6]$$

$$2S_2^{-\cdot} \rightleftharpoons S_4^{2-} \quad [7]$$

$$S_4^{2-} + S_2 \rightleftharpoons S_6^{2-} \quad [8]$$

$$S_6^{2-} + S_2 \rightleftharpoons S_8^{2-} \quad [9]$$

The polysulfides generated from the reduction of sulfur in nonaqueous solvents by various alkali metals were also reported.[17] A yellow solution obtained from reduction of sulfur in tetrahydrofuran by Li, Na, K, or Cs showed an absorption peak at 435, 420, 445, or 460 nm, respectively, and the species was interpreted to be tetrasulfide dianion, S_4^{2-}. A blue solution formed from the addition of hexamethyl phosphoramide to the yellow solution showed an absorption peak at 620 nm, which was assigned to $S_3^{-\cdot}$ radical, which was confirmed by ESR experiments.

We also published a reduction mechanism of sulfur in dimethyl sulfoxide solutions studied by *in situ* spectroelectrochemical techniques.[8] In the study, we reported S_8^{2-}, S_6^{2-}, S_4^{2-}, $S_3^{-\cdot}$, and S_3^{2-} species as reduction products generated at the first reduction step, which were essentially identical to those formed at the second reduction wave. Final products generated at the second wave were reported to be S_3^{2-} and S_4^{2-}. We provided spectroscopic evidence of a previously unreported absorption band observed at 770 nm as $S_4^{-\cdot}$ species. However, Gaillard and Levillain[10] pointed out that our study did not shed much light on the time dependencies of these

species due to the lack of a fast spectrograph. Nonetheless, Levillain *et al.* addressed only the earlier phase reactions of sulfur reduction to explain the cyclic voltammetric current shapes employing digital simulation without presenting the whole picture of the reaction. We herewith present the overall picture of the reaction mechanism for sulfur reduction and evaluate the system in terms of chemical reversibility, which is an important feature for a reaction as a battery reactant.

In the present study, we use a spectrograph equipped with a charge coupled device (CCD) array detector for *in situ* spectroelectrochemical studies to obtain absorption spectra in real-time. The time for recording a full frame spectrum for an entire spectral range is 25 ms. Using this spectroelectrochemical system, we investigated time as well as potential dependencies of the intermediate species generated during the electrochemical reduction of sulfur in DMF. Based on the spectroscopic behaviors of polysulfide anions, a more realistic reduction mechanism is proposed.

Experimental

All the samples were handled in a glove box filled with argon to avoid contamination by moisture and oxygen. Sulfur, lithium trifluoromethane sulfonate, and DMF (all ACS reagent grades) were obtained from Aldrich. DMF was used after fractional distillation under reduced pressure.

A Princeton Applied Research model 273A potentiostat-galvanostat was used for electrochemical experiments. For spectroelectrochemical measurements, a near normal incident reflectance spectroelectrochemical (NNIRS) setup,[22-24] assembled using a bifurcated quartz fiber optical probe, was employed with an Oriel 77540 spectrograph equipped with a CCD detector. The spectra shown were obtained by integrating the detector signals from as few times as 2 to as many times as 40 depending on how noisy the signals were. Although we show only a limited number of selected representative spectra, we recorded and examined hundreds of spectra. The complex spectra were deconvoluted into component bands by curve fitting with a Microcal Origin 6.0 program. A reflective platinum or glassy carbon disk electrode, polished to a mirror finish with alumina powder (down to 0.3 μm), was served as a working electrode as well as mirror for spectroelectrochemical measurements. A silver wire was used as a pseudoreference electrode, while a platinum spiral wire was employed as a counter electrode. An electrochemical cell housing all these three electrodes was used for electrochemical and spectroelectrochemical measurements. The reflective working electrode has its surface facing up, which makes it a bulk cell as the electrogenerated species are exposed to the bulk of the solution.[22] It becomes a thin layer cell when a quartz slide with a larger area than that of the working electrode covers the surface of the reflective working electrode, which makes the solution confined within the two walls.[23] This cell has a cell thickness of about 30 μm.[23] Details of the construction of these cells have been described elsewhere.[22,23] For the potential step experiments to record spectra, the potential was stepped to a desired value from an open-circuit potential, which fell in the range of −0.30 to −0.40 V, with −0.35 V observed most frequently.

Results and Discussion

Figure 1 shows a CV obtained at (a) platinum and (b) glassy carbon electrodes for reduction of 3 mM sulfur in DMF containing 1.0 M lithium trifluoromethane sulfonate (LiCF$_3$SO$_3$) as a supporting electrolyte. The shape of the CV recorded in this study is in excellent agreement with those reported previously,[8,10] where a dimethylsulfoxide solution containing tetra-*n*-butylammonium perchlorate was used. We clearly see from the CVs that sulfur reduction is much more reversible at glassy carbon electrodes compared to that at platinum electrodes; however, we used a platinum electrode due to its better reflectivity for the spectroelectrochemical study. Highly hydrophobic compounds usually show quasi-reversible electrochemical behaviors at metal electrodes, whereas their electrochemical reactions are more reversible at glassy carbon electrodes due to
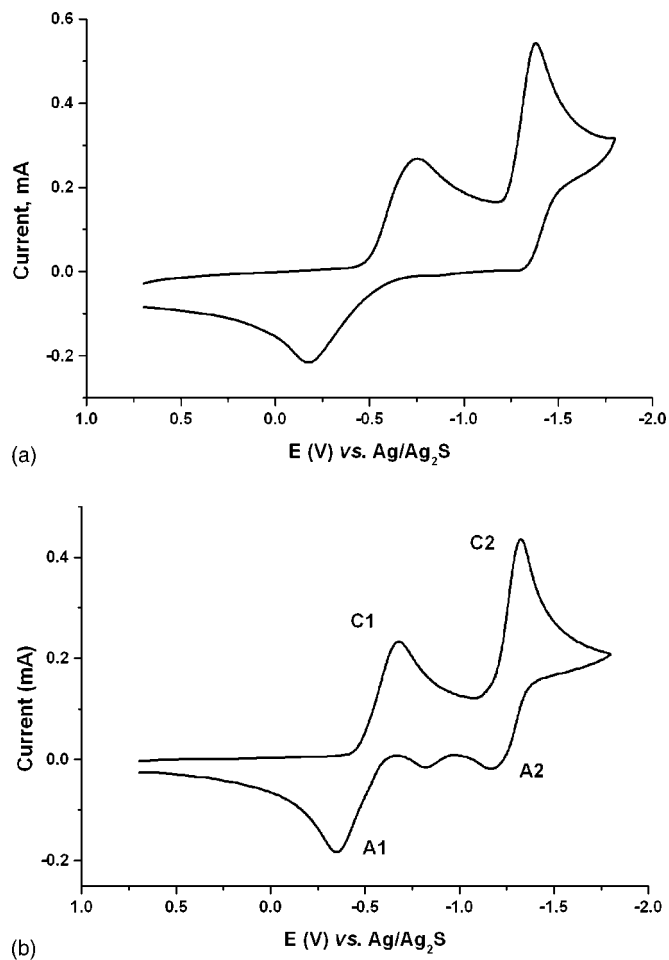

(a)

(b)

Figure 1. CV for reduction of 3 mM sulfur at (a) platinum and (b) glassy carbon electrodes in a DMF solution containing 1.0 M LiCF$_3$SO$_3$ at a scan rate of 50 mV/s.

their higher affinities. Gaillard and Levillain[10] emphasized the importance of what they called a prewave in their CVs and claimed from their time-resolved spectroelectrochemical studies that it was observed because of electrochemical reduction of S$_8$ to S$_8^{2-}$ and/or to S$_8^-$. They also claimed that the formation of S$_3^-$ and S$_6^{2-}$ was also obtained at the reduction prewave, *i.e.*, reduction of S$_4^-$ and S$_8^{2-}$, rather than the disproportionation reaction of S$_8^{2-}$ in our report;[8] however, we could not see the prewave in our CV that they claimed they had seen. What they called the prewave is actually a small reduction wave observed between two major reduction waves, C$_1$ and C$_2$, in Fig. 1b, which was attributed to that of impurities by Badoz-Lambling *et al.*[25] However, we have not observed it in a well-dried, clean solution.

Figure 2 shows a series of spectra recorded when the electrolysis of sulfur is carried out in a bulk solution at −0.60 V, near the half peak potential of the first reduction wave. Absorption peaks begin to develop at 360 and about 490 nm, 6 s after the potential step (Fig. 2a). The species observed at these wavelengths must be the first product related to S$_8^{2-}$. In our previous study,[8] the absorption peaks observed at these two wavelengths were assigned to S$_8^{2-}$, because the absorbance at 490 nm was observed together with that at 355 nm from the very beginning of the experiment. At 9 s, an absorption band at 600 nm begins to develop as a shoulder, and the 355 nm band becomes the highest. As the electrolysis proceeds, the peaks at 355, 490, and 600 nm grow, and the one at 490 nm becomes dominant when the time is longer than 150 s. However, it was noticed
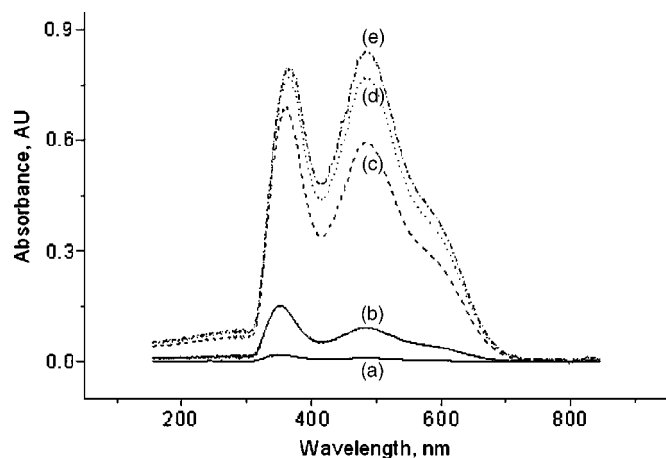
Figure 2. Spectra recorded during electrolysis of 3.0 mM sulfur at −0.6 V in DMF in a bulk cell: (a) 6, (b) 9, (c) 75, (d) 150, and (e) 300 s after the potential step.

from the spectra recorded at −0.2 V (not shown) that the absorption peak at 355 nm is the highest, with those bands at 490 and 600 nm never dominant even at a long electrolysis time.

Figure 3 shows the change in absorbance at the three wavelengths as a function of time ($1 \sim 300$ s) during and after electrolysis. Until about 90 s of electrolysis, the increase in absorbance at 355 nm is faster than that at 490 nm. Thereafter, the absorbance at 355 nm stays constant, whereas that at 490 nm continues to increase, although its rate of increase is small. The reason the rise in absorbance stopped after certain time is past is perhaps due to the natural convection. These changes indicate that the species responsible for absorbance at 355 and 490 nm are not identical and the species absorbing at 490 nm may also be produced from that at 355 nm through an equilibrium reaction. Also noticeable is that the 490 nm band decreases faster than that at 355 nm when the circuit is opened. This is consistent with the equilibrium reaction of the species absorbing at 490 nm back to that at 355 nm, because the faster decrease in the 490 nm band (rate of decay 0.014 s^{-1}) may be related to an increase in the 355 nm band, which makes the decay of the 355 nm band (decay rate 0.011 s^{-1}) a little slower. The first-order decay rates were calculated from the $\ln[A(t)]$ *vs. t* data.

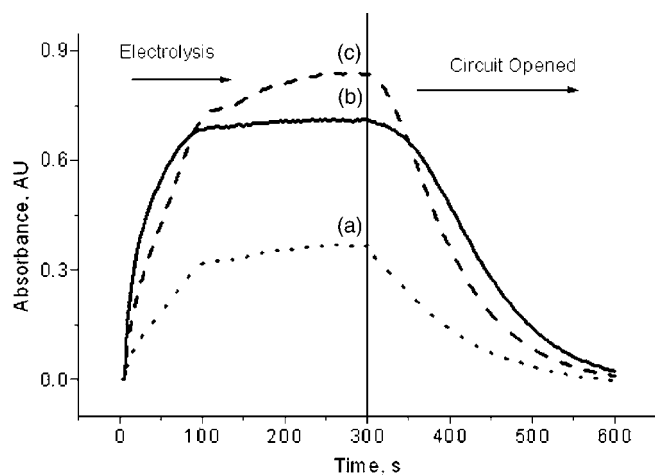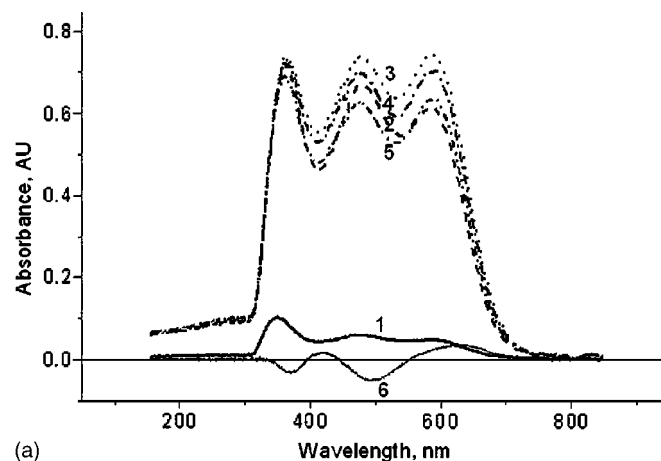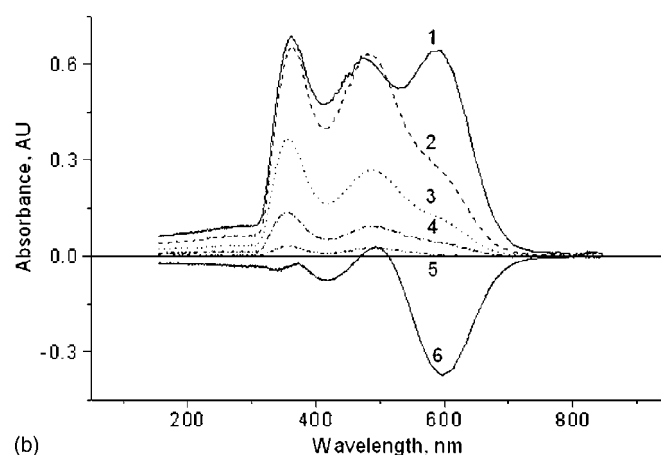Figure 4 shows (a) spectra obtained during (a) and after (b) the

Figure 3. Absorbance *vs.* time plots obtained from the spectra recorded during the first 300 s of electrolysis and the next 300 s after the circuit is opened: (a) 600, (b) 350, and (c) 490 nm. The data were taken from the same experiments as in Fig. 2.

Figure 4. (a) Spectra obtained during electrolysis of 3.0 mM sulfur at −1.3 V in DMF in a bulk cell: (1) 3, (2) 75, (3) 150, (4) 225, and (5) 300 s after the potential step, and (6) difference spectrum obtained from those shown in (5) and (2). (b) Spectra recorded for the solution used in (a): (1) 3, (2) 75, (3) 150, (4) 225, and (5) 300 s after the circuit was opened, and (6) the difference spectrum obtained from those shown in (2) and (1).

electrolysis at −1.3 V (near the vertex potential of the second reduction wave). As soon as the potential is stepped, we observe the absorption bands at 355, 490, and 600 nm (Fig. 4a-1). At this potential, we observe only moderate changes in absorbance of these bands without considerable wavelength shifts even after a long period of electrolysis (Fig. 4a-2 and a-3). Figure 4a-6 shows the difference spectrum between those obtained at 300 and 75 s of electrolysis. It shows that the absorption bands at 420 and 600 nm increase, whereas those at 355 and 490 nm decrease. These changes indicate that the species absorbing at 420 and 600 nm are generated at the expense of the species observed at 355 and 490 nm during electrolysis. In other words, we observe a new species absorbing at 420 nm at this potential, which was not seen at the first CV wave. This observation is somewhat different from that in our previous results,[8] where the products obtained in the first wave were not significantly different from those generated at the second wave. The product observed at 420 nm must be a highly reduced species, because the electrolysis was carried out at a higher reduction potential.

Upon opening the circuit for this electrolyzed solution, we obtain spectra shown in Fig. 4b-1 through 4b-5. Figure 4b-6 is the difference spectrum obtained from those between 75 and 3 s after the circuit is opened. In this figure, we clearly see that the disappearance of the species observed at 600 nm is faster than any other species. Thus, the species observed at 600 nm is not as stable as the other species. Due to its instability, this species was assigned to a radical
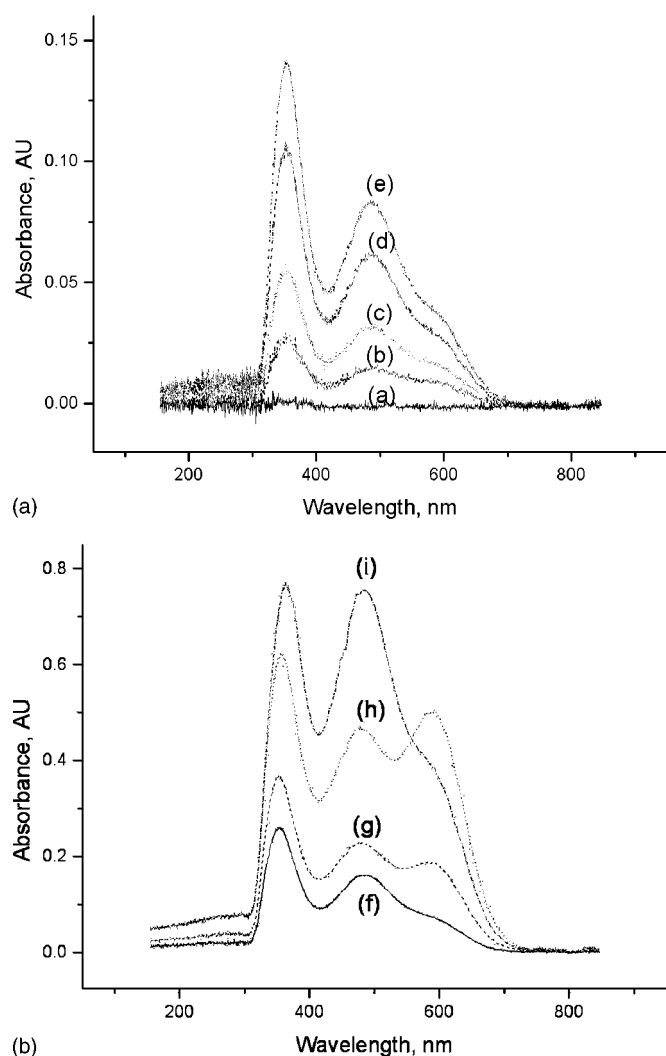
Figure 5. Spectra obtained during the CV scan for the reduction of sulfur in a DMF bulk solution at a scan rate of 50 mV/s: (top) (a) -0.150, (b) -0.225, (c) -0.275, (d) -0.350, and (e) -0.400, and (bottom) (f) -0.600, (g) -1.200, (h) -0.800, and (i) $+0.100$ V (at the first oxidation wave on CV). Scan rate 50 mV/s. Note that potentials at (f) and (g) are at the first and second reduction CV peaks and (h) and (i) are during the reversal scan.

anion, $S_3^{-\cdot}$, in our previous study;[8] this was also confirmed by ESR studies by others.[14,17]

The potential dependencies of the species generated in the bulk cell studied by recording spectra during the potential scan at 50 mV/s are shown in Fig. 5. Although the spectra were recorded every 50 mV or 1 s, only the spectra recorded at a few selected potentials are displayed here. We begin to see a hint of the first spectrum, when the scanned potential reaches -0.15 V, which appears to consist of a single band at 355 nm as shown in Fig. 5a. Thus, the species observed at 355 nm seems to be the first product generated upon electrochemical reduction. Soon after the potential is scanned further down, we see the bands at 355 and 490 nm with a shoulder at 600 nm (Fig. 5b). The bands at these two wavelengths (355 and 490 nm) were assigned to an identical species, *i.e.*, S_8^{2-}, in our previous study.[8] However, the species observed at 355 and 490 nm must be different for two reasons: (*i*) the band at 355 nm is observed at a less negative potential than that at 490 nm, as can be seen in Fig. 5a, and (*ii*) their rise and decay were shown to be different (Fig. 3). The structure of S_8^{2-} can be either a cyclic (S_{8c}^{2-}) or linear chain form (S_{8l}^{2-}).[16] Based on the observation of the single band at 355 nm, we

assign this species to S_{8c}^{2-} generated from the electrochemical reduction of closed form of S_8, which is known to be the most stable form of elemental sulfur.[9,20] The S_{8c}^{2-} species would be generated directly from the two-electron reduction of chain form S_8

$$S_{8c} + 2e^- \rightleftharpoons S_{8c}^{2-} \qquad [10]$$
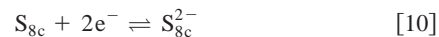
or via a fast second electron transfer to $S_{8c}^{-\cdot}$ generated from Reaction 1 as Levillain *et al.* claimed according to

$$S_{8c}^{-\cdot} + e^- \rightleftharpoons S_{8c}^{2-} \qquad [11]$$

This scenario is quite reasonable because $S_{8c}^{-\cdot}$ would be a predominant species due to the small equilibrium constant of K_1 in Reaction 1. Then the species observed at 490 nm must be the secondary product formed from the series of chemical or electrochemical reactions according to Reactions 2–4 if Levillain *et al.*'s mechanism[14] is correct. The 355 nm band cannot be assigned to $S_{8c}^{-\cdot}$ (radical anion) because its transition energy must be much smaller (see below). The assumption employed in our assignment is that the transition energy would be higher for the cyclic form than for the linear form, because the electrons on the highest occupied molecular orbital (HOMO) would be more tightly held in molecules of the cyclic shape. In no studies have the two bands been assigned to other species than S_8^{2-} such as $S_8^{-\cdot}$, whether it is of chain or linear form.[8,10]

It has been reported that the stable structures of S_3^{2-}, S_4^{2-}, S_6^{2-}, and S_8^{2-} take the linear form, whereas those of elemental sulfur and $S_8^{-\cdot}$ anion are cyclic.[16,20,21] Because the linear chain shape is more stable than the cyclic form of S_8^{2-}, the primary product would undergo a ring-opening reaction to a more stable structure, *i.e.*, S_{8l}^{2-}, as soon as the species is generated. We would thus expect an equilibrium reaction

$$S_{8c}^{2-} \rightleftharpoons S_{8l}^{2-} \qquad [12]$$

from the list of possible reactions in the sulfur reduction mechanism, which has not been considered by Levillain *et al.* in their digital simulation.[10]

As the reduction potential becomes more negative (Fig. 5b-e), the intensities of all the bands at 355, 490, and 600 nm increase along with that at about 280 nm. As shown in Fig. 5g, all the absorption bands increase when the scanned potential is in the range of the second reduction wave. However, when the potential is reversed and reaches the second oxidation wave of the CV (Fig. 5h), all the bands increase even further, with a particularly fast increase noticeable in the 600 nm band. As the potential is scanned further back to the first oxidation wave (Fig. 5i), the bands at 280, 355, and 490 nm maintain large increments while that at 600 nm decreases.

While the spectra recorded as a function of time and/or potential may give a good picture of what is going on during electrolysis at a given potential or at varied potentials, their interpretation is not always straightforward because the species generated may undergo reactions with unreduced sulfur species, solvents, or other electrogenerated species. We therefore ran spectroelectrochemical experiments in a thin-layer electrochemical cell (TLEC) in which an exhaustive electrolysis is completed within a short period. Figure 6a shows the spectra obtained while 3 mM sulfur is electrolyzed at -0.70 V in DMF in a thin layer cell (at around the peak potential of the first reduction wave on CV in the TLEC). We observe an absorption peak at 355 nm and a broad band at about 490 nm at the beginning of the electrolysis, which we assigned to the ring and linear forms of S_8^{2-} generated via Reactions 10 and/or 11. The absorbance at 355 nm increases until 3.25 s (Fig. 6a, line 2), and the band at 490 nm shifts to 450 nm with a shoulder at about 600 nm beginning to appear. Thus, the species at 450 and 600 nm are the secondary products, coming from S_{8l}^{2-}. The absorbance shows small increments at 355 and 450 nm at 3.75 s, but the band at 600 nm
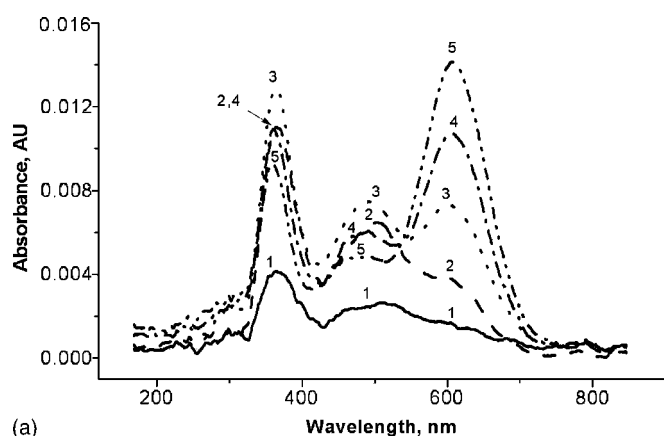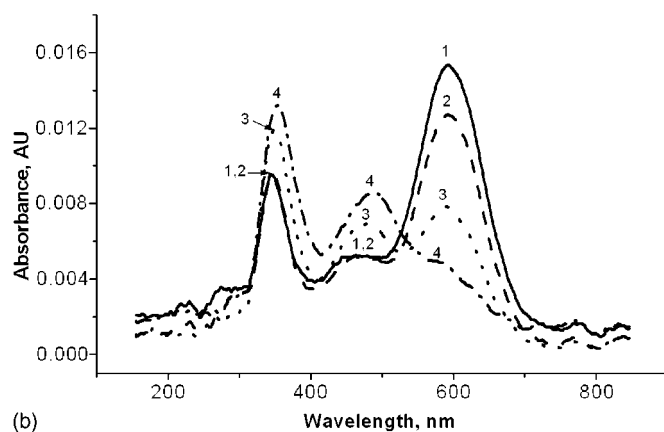
Figure 6. (a) Spectra obtained during electrolysis of 3.0 mM sulfur in DMF at −0.70 V in a thin-layer cell: (1) 2.75, (2) 3.25, (3) 3.75, (4) 5, and (5) 10 s after the potential step, (b) Spectra obtained from the same solution as for (a): (1) 0.25, (2) 3, (3) 5, and (4) 20 s after the circuit is opened. The spectra shown here have been smoothed by a 40-point digital smoothing procedure.

Figure 7. (a) Spectra obtained during electrolysis of 3.0 mM sulfur in DMF at −1.25 V in a thin layer cell: (1) 0.25, (2) 5, (3) 10, (4) 15, and (5) 20 s after the potential step; and (b) spectra obtained from the same solution used for spectra shown in (a): (1) 0.25, (2) 20, (3) 40, (4) 60, and (5) 80 s after the circuit was opened.

shows a large increase, becoming a major band, while the one at 450 nm decreases (Fig. 6a, line 3). Also, there is an isosbestic point at about 535 nm, suggesting that the species at 600 nm, *i.e.*, $S_3^{-\cdot}$, is generated at the expense of that at 450 nm. In other words, the species absorbing at 450 nm is derived from the one at 490 nm, which also accompanies the increase in the 280 nm band, which is due to dianions of shorter chains and free sulfur (S_8).[8] We thus assign the band at 450 nm to S_6^{2-} formed via a reaction
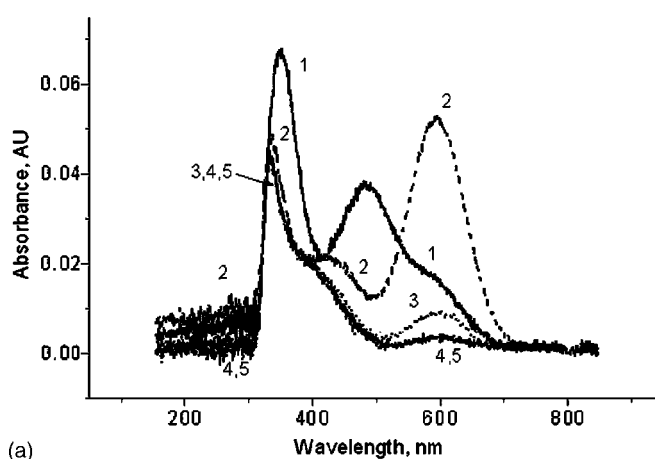
$$S_{81}^{2-} \rightleftharpoons S_6^{2-} + 1/4 S_{8c}. \qquad [13]$$
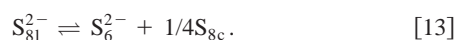
The homolytic dissociation of S_6^{2-} thus formed to $S_3^{-\cdot}$ according to
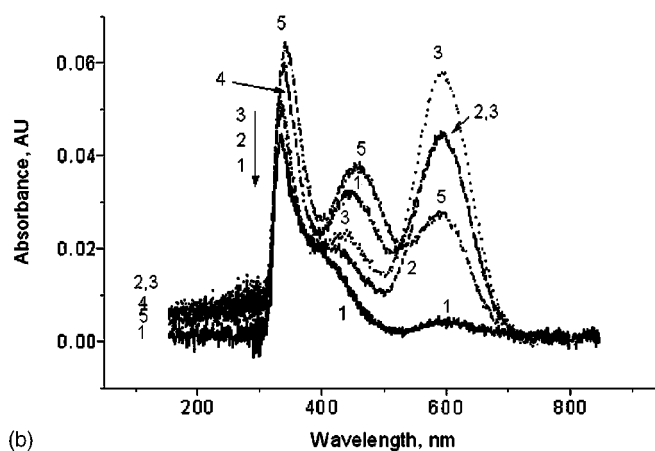
$$S_6^{2-} \rightleftharpoons 2S_3^{-\cdot} \qquad [14]$$

explains the large increase in the 600 nm band. Thus, we confirm the generation of ring and linear forms of S_8^{2-}, S_6^{2-}, and $S_3^{-\cdot}$ during the electrolysis at −0.70 V in the TLEC.

When this solution was allowed to relax with its circuit opened (Fig. 6b), the 355 (S_{8c}^{2-}) and 450 nm (S_6^{2-}) bands stayed about constant while the 600 nm band ($S_3^{-\cdot}$) decreased for the first 3 s. Thereafter, the 355 nm band increased while the 450 nm band shifted back to 490 nm (S_{81}^{2-}) with its absorbance increasing for next 20 s. In the mean time, the 600 nm band decreased fast and then disappeared. The 355 and 490 nm bands reached steady values after 20 s until the end of the experiment. Now we see that the 355 nm (S_{8c}^{2-}) and 490 nm (S_{81}^{2-}) bands were regenerated upon opening the circuit for 20 s. From the spectral changes observed here, we con-

clude that the sulfur system in a thin layer cell is chemically reversible and thus, the species S_6^{2-} (450 nm) and $S_3^{-\cdot}$ (600 nm) are intermediates in this sequence of reactions.

Figure 7 shows the spectra recorded at −1.25 V (the second reduction wave on the CV) in the TLEC. Here we see that the species such as S_{8c}^{2-} (355 nm), S_{81}^{2-} (490 nm), and $S_3^{-\cdot}$ (600 nm) are generated from the beginning of electrolysis. In this case, $S_3^{-\cdot}$ must be generated directly from S_{81}^{2-} species (490 nm) via Reaction 15 rather than reactions 13 and 14,

$$S_{81}^{2-} \rightleftharpoons 2S_3^{-\cdot} + 1/4 S_{8c}. \qquad [15]$$

The changes observed thereafter at longer electrolysis time is summarized as following. Between 0.25 and 4 s (not shown), the 600 nm band grows significantly while the 490 and 355 nm bands undergo decreases in their absorbance values and spectral shifts to 438 and 330 nm, respectively. During this period, the absorbance at 280 nm increases as well. As a result, the spectrum takes the form shown in Fig. 7a-2 at 5 s. At 10 s (Fig. 7a-3), the 438 band undergoes a further decrease in its intensity and an additional spectral shift to 420 nm, while the 600 nm peak is suppressed quite a bit. Eventually, the 600 nm band is almost gone while the other bands stay almost constant (Fig. 7a-4 and 5).

These observations indicate that a number of reduction products are produced at this potential under the rather rigorously reducing condition. For the assignments of spectral bands, we used the spec-

Table I. Spectral assignments for the bands observed in this study.[a]

S^{2-}	S_2^{2-}	S_3^{2-}	S_4^{2-}	S_5^{2-}	S_6^{2-}	S_7^{2-}	S_{8l}^{2-}	S_{8c}^{2-}	$S_3^{-\cdot}$	$S_4^{-\cdot}$
250	280	334	420	435	340, 450	470	490	355	600	~700

[a] Wavelengths in nanometers.

troelectrochemical behaviors and a general principle based on the relative energies required for electronic transitions for the intermediate species or reduction products.[8] The principle can be stated as: (*i*) the anion radicals and dianions with higher electron to sulfur ratios have their absorbance at higher energies (shorter wavelengths), (*ii*) the dianions require larger energies than their anion radical counterparts, and (*iii*) a dianion of the linear chain requires less energy than its cyclic counterpart. The spectral assignments according to these principles for the bands observed in this study are listed in Table 1. These assignments explain the observations in this study very well.
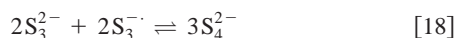
An intermediate species, $S_3^{-\cdot}$, produced through Reactions 14 and 15 following the first electrochemical reaction, undergoes further reduction to its product, S_3^{2-}, at this potential

$$S_3^{-\cdot} + e^- \rightleftharpoons S_3^{2-} \qquad [16]$$

which absorbs at 330 nm. The spectral change observed between 4 and 5 s of electrolysis indicates that S_{8l}^{2-} is reduced further to S_4^{2-} according to

$$S_{8l}^{2-} + 2e^- \rightleftharpoons 2S_4^{2-} \qquad [17]$$

and

$$2S_3^{2-} + 2S_3^{-\cdot} \rightleftharpoons 3S_4^{2-} \qquad [18]$$

which absorbs at 420 nm. This assignment is consistent with not only our observation but also Tobishima *et al.*'s report,[17] in which sulfur was chemically reduced to S_4^{2-} with alkali metals such as Li, Na, K, or Cs in tetrahydrofuran. Also, the reaction

$$2S_4^{2-} \rightleftharpoons 2S_3^{-\cdot} + S_2^{2-} \qquad [19]$$
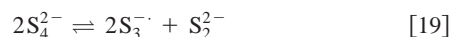
explains the reduction in absorbance at 420 nm (S_4^{2-}) and the increase in bands at 600 ($S_3^{-\cdot}$) and 280 nm (S_2^{2-}), between 0.25 and 5 s of electrolysis. The decrease in most bands after 5 s is explained by the reaction

$$3S_2^{2-} \rightleftharpoons 2S^{2-} + S_4^{2-} \qquad [20]$$
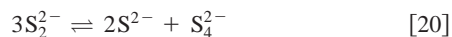
where S^{2-} absorbs below 280 nm. Finally, the observation of the 438 nm peak, assigned to S_5^{2-}, is consistent with the reaction

$$2S_3^{2-} \rightleftharpoons S_5^{2-} + S^{2-} \qquad [21]$$

The absorption band at about 250 nm is attributed to S^{2-}; the presence of S^{2-} and S_2^{2-} in the reduction products of sulfur was confirmed independently by recording the X-ray diffraction (XRD) spectra of the products obtained from exhaustive reduction of sulfur. Similar observations have been reported in the literature.[6,7,26] At longer electrolysis times (Fig. 7b-3 to 7b-5), all the absorption peaks decrease until the time reaches 15 s when the electrolysis is completed.

From the spectroelectrochemical behavior in a thin-layer cell at −1.25 V, we conclude that considerable amounts of $S_3^{-\cdot}$ species are generated at the beginning via the consumption of S_{8c}^{2-} and S_{8l}^{2-}. Later, more reduced species, S_3^{2-}, S_4^{2-}, and S_5^{2-}, observed at 330, 420, and 438 nm, are obtained. The generation of S_2^{2-} and S^{2-} is also confirmed by absorption bands in the 250–280 nm region.
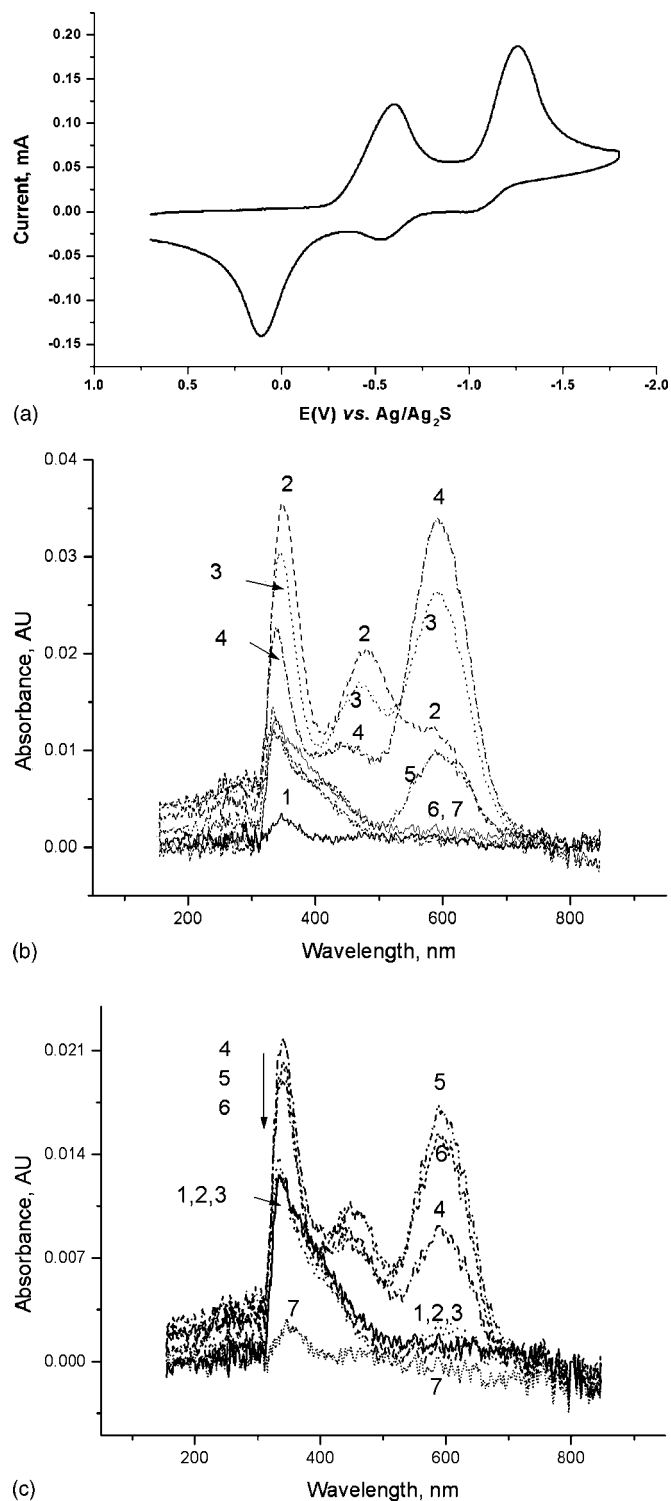

Figure 8. (a) CV obtained for a 3.0 mM sulfur in the thin layer cell at 50 mV/s. (b) Spectra obtained for 3 mM sulfur in DMF in the TLEC during the forward scan at (1) −0.275, (2) −0.600, (3) −0.800, (4) −1.000, (5) −1.250, (6) −1.600, and (7) −1.750 V, and (c) during the reverse scan at (1) −1.750, (2) −1.275, (3) −0.750, (4) −0.500, (5) −0.350, (6) −0.150, and (7) +0.100 V.

Figure 7b shows the spectra obtained from the same solution when it was allowed to relax. Examination of the spectral changes shown in Fig. 7b leads to the conclusion that the system is chemically reversible.

Figure 8 shows a CV recorded in the TLEC (a) and the potential

dependencies of the spectral bands studied by concurrently recording spectra during the potentiodynamic scan (b and c). Until the potential reaches the first reduction peak (Fig. 8b-1,2), absorption peaks are observed at 355, 490, and 600 nm, indicating that S_{8c}^{2-} (355 nm) is first generated (Reaction 10), followed by its equilibrium to S_{81}^{2-} (Reaction 12 and eventually to $S_3^{-\cdot}$ (Reaction 14), as expected. In the diffusion-limited region of the first wave, *i.e.*, -0.625 to -0.8 V, the 600 nm peak and a broad band at 250-280 nm show increases, whereas the 355 and 490 nm bands show decreases (Fig. 8b-3). This trend continues up to -1.0 V, indicating that Reaction 15 is a major path for the following chemical reaction of S_{81}^{2-}. Also, the spectral shift of the 490 nm band to 470 nm is observed at -0.80 V (Fig. 8b-3), suggesting that the dissociation of S_{81}^{2-} to its smaller fragments takes place. Based on the combination of relative energetics and spectroscopic behavior described, we assign this band to S_7^{2-} species, which is formed from the reaction

$$S_{81}^{2-} \rightleftharpoons S_7^{2-} + 1/8 S_{8c} \qquad [22]$$

In the potential region of -0.9 to -1.0 V, large increases in the 600 and 250–280 nm bands are noted and a further spectral shift of the 470 nm band to 450 nm is observed, which we attribute to the formation of S_6^{2-} according to the reaction

$$S_7^{2-} \rightleftharpoons S_6^{2-} + 1/8 S_{8c} \qquad [23]$$

and/or Reaction 13. When the potential reaches the second reduction wave, all these species are shown to be reduced, as shown in Fig. 8b-5, 6, and 7. At the same time, the 450 nm peak undergoes another wavelength shift to 420 nm (S_4^{2-}), becoming a shoulder of the absorption peak at 330 nm (S_3^{2-}), which itself has been shifted from 355 nm. Therefore, S_3^{2-} and S_4^{2-} are produced as reduction products of $S_3^{-\cdot}$ and S_{81}^{2-} according to Reactions 16 and 17 at the second reduction wave, as stated previously. Also, a reaction

$$S_4^{2-} \rightleftharpoons S_3^{2-} + 1/8 S_{8c} \qquad [24]$$

appears to occur along with Reaction 16 for generation of S_3^{2-}.

The spectra recorded during the reversal scan shown in Fig. 8c indicate that the sulfur reduction is chemically reversible although the reaction paths are complicated. In the cathodic potential region -1.750 to -0.750 V (Fig. 8c-1 to 3), high absorbance is observed in the 250–300 nm region, suggesting that small amounts of S_2^{2-} or S^{2-} species are produced. In the potential region of -0.475 to -0.350 V, the spectral shift of 420 back to 450 nm was observed without significant changes in absorbance due to the regeneration of S_6^{2-} species. The observation in this potential region can be explained by Reactions 19 and 20 as well as

$$2 S_4^{2-} \rightleftharpoons S_6^{2-} + S_2^{2-} \qquad [25]$$

From the potential dependencies carried out in the TLEC, we observe a new species, S_7^{2-} (470 nm), which is generated from S_{81}^{2-} (490 nm) in the first reduction step according to Reaction 22, which then undergoes a rapid change to S_6^{2-} (450 nm) via Reaction 23. We believe that S_7^{2-} species is not stable in DMF as its absorption did not last long. Also, the generation of relatively highly reduced species, S_3^{2-} and S_4^{2-}, was confirmed only at the second reduction step. These species were stable until the potential reaches the first oxidation step during the reverse scan. During reduction at the second electron-transfer step, the highly reduced species, S_2^{2-} or S^{2-}, were shown to be generated as by-products of the reactions. This would be a reaction path to form insoluble Li_2S_2 or Li_2S in practical lithium/sulfur batteries.[27-29] These compounds have been known to cause poor cycle lives as well as cell capacities due to their poor reversibility.[17,27-29]

Conclusion

In this study, we carried out detailed real-time *in situ* spectroelectrochemical studies in bulk as well as thin layer cells. In DMF, we observed only S_{8c}^{2-}, S_{81}^{2-}, and $S_3^{-\cdot}$ species from the first electron-transfer step, whereas S_4^{2-} was observed at the second step in addition to the above-mentioned species. Of these, S_{8c}^{2-}, S_{81}^{2-}, $S_3^{-\cdot}$, and S_4^{2-} were the relatively stable species in DMF in our experimental time scale. In general, S_8, S_8^{2-}, S_6^{2-}, and $S_3^{-\cdot}$ are known to be stable in dipolar aprotic media such as DMF, dimethyl sulfoxide, dimethylaniline, and acetonitrile.[9]

In TLEC experiments, we obtained clear information on the electrogenerated species due to its capability of exhaustive electrolysis. We observed new species attributable to S_5^{2-} (437 nm) and S_7^{2-} (470 nm), which were relatively unstable in DMF. Also, the species observed at the first and the second reduction steps were not the same. We observed S_3^{2-} and S_4^{2-} only from the second reduction step via further reduction of corresponding anion radicals such as $S_3^{-\cdot}$ and $S_4^{-\cdot}$, reductive breakage of longer chain ions (Reaction 17), and recombination of smaller species (Reactions 18–20). The difference between the observations obtained from bulk and thin layer cells results from the presence and absence of following reactions of electrogenerated species with unreduced sulfur, reduced sulfur species, and solvent molecules. The reactions such as disproportination take place thanks to the sustained availability of reactants after the electron-transfer products are produced in the bulk cell. In the thin-layer cell, however, the primary reduced species undergo further reduction to more highly reduced species.

In this study, we have clearly shown that the species absorbing at 355 and 490 nm are generated sequentially, contrary to the thoughts in previous reports. We also made complete assignments of spectral bands thanks to better spectral resolution and the real-time recording capability of the spectrometer we used. Finally, we should point out that the sulfur reduction is chemically reversible, although its following reactions are rather complex and many equilibrium reactions occur after the electron transfer. The following reactions after the second electron transfer explain smaller anodic CV peaks during the reversal scans than their cathodic counterparts in the CVs shown in Fig. 1. However, this chemical reversibility is important as a cathode reaction for secondary battery applications, although small amounts of S^{2-} and S_2^{2-} formed during the deep charging cycles would make the battery efficiency lower than theoretically expected.

References

1. J. Broadhead and T. Skotheim, *J. Power Sources*, **65**, 213 (1997).
2. D. Marmorstein, T. H. Yu, K. A. Striebel, F. R. McLarnon, J. Hou, and E. J. Cairns, *J. Power Sources*, **89**, 219 (2000).
3. M. V. Merritt and D. T. Sawyer, *Inorg. Chem.*, **9**, 211 (1970).
4. R. P. Martin and D. T. Sawyer, *Inorg. Chem.*, **11**, 2644 (1972).
5. R. P. Martin, W. H. Doub, Jr., J. L. Roberts, Jr., and D. T. Sawyer, *Inorg. Chem.*, **12**, 1921 (1973).
6. P. Dubois, J. P. Lelieur, and G. Lepoutre, *Inorg. Chem.*, **27**, 73 (1988).
7. P. Dubois, J. P. Lelieur, and G. Lepoutre, *Inorg. Chem.*, **27**, 1883 (1988).
8. B.-S. Kim and S.-M. Park, *J. Electrochem. Soc.*, **140**, 115 (1993).
9. G. Bosser and J. Paris, *New J. Chem.*, **19**, 391 (1995), and references therein.
10. F. Gaillard and E. Levillain, *J. Electroanal. Chem.*, **398**, 77 (1995).
11. E. Levillain, A. Demortier, and J. P. Lelieur, *J. Electroanal. Chem.*, **394**, 103 (1995).
12. A. Demortier and J. P. Lelieur, *J. Electroanal. Chem.*, **394**, 205 (1995).
13. E. Levillain, F. Gaillard, A. Demortier, and J. P. Lelieur, *J. Electroanal. Chem.*, **405**, 85 (1996).

14. P. Leghie, E. Levillain, J.-P. Lelieur, and A. Lorriaux, *New J. Chem.,* **20**, 1121 (1996).
15. P. Leghie, E. Levillain, and J. P. Lelieur, *New J. Chem.,* **20**, 1121 (1996).
16. E. Levillain, F. Gaillard, P. Leghie, A. Demortier, and J. P. Lelieur, *J. Electroanal. Chem.,* **420**, 167 (1997).
17. S. I. Tobishima, H. Yamamoto, and M. Matsuda, *Electrochim. Acta,* **42**, 1019 (1997).
18. F. Gaillard, E. Levillain, and J. P. Lelieur, *J. Electroanal. Chem.,* **432**, 129 (1997).
19. E. Levillain, F. Gaillard, and J. P. Lelieur, *J. Electroanal. Chem.,* **440**, 243 (1997).
20. D. R. Sahalub, A. E. Foti, and V. H. Smith, Jr., *J. Am. Chem. Soc.,* **100**, 7847 (1978).
21. S. Hunsicker, R. O. Jones, and G. Gantefor, *J. Chem. Phys.,* **102**, 5917 (1995).
22. C.-H. Pyun and S.-M. Park, *Anal. Chem.,* **58**, 251 (1986).
23. C. Zhang and S.-M. Park, *Anal. Chem.,* **60**, 1639 (1988).
24. C. Zhang and S.-M. Park, *Bull. Korean Chem. Soc.,* **10**, 302 (1989).
25. J. Badoz-Lambling, R. Bonnaterre, G. Cauquis, M. Delmar, and G. Demange, *Electrochim. Acta,* **21**, 119 (1976).
26. P. Leghié, J.-P. Lelieur, and E. Levillain, *Electrochem. Commun.,* **4**, 406 (2002).
27. B. H. Jeon, J. H. Yeon, K. M. Kim, and I. J. Chung, *J. Power Sources,* **109**, 89 (2002).
28. R. D. Rauth, K. M. Abraham, G. F. Pearson, J. K. Surprenant, and S. B. Brummer, *J. Electrochem. Soc.,* **126**, 523 (1979).
29. E. Peled, A. Gorenshtein, M. Segal, and Y. Sternberg, *J. Power Sources,* **26**, 269 (1989).